

HCO⁺ AND HCN J=3-2 ABSORPTION TOWARD THE CENTER OF CENTAURUS A

SÉBASTIEN MULLER¹ & DINH-V-TRUNG^{1,2}
Draft version October 24, 2018

ABSTRACT

We have investigated the presence of dense gas toward the radio source Cen A by looking at the absorption of the HCO⁺ and HCN (3-2) lines in front of the bright continuum source with the Submillimeter Array. We detect narrow HCO⁺ (3-2) absorption, and tentatively HCN (3-2), close to the systemic velocity. For both molecules, the $J = 3 - 2$ absorption is much weaker than for the $J = 1 - 0$ line. From simple excitation analysis, we conclude that the gas density is on the order of a few 10^4 cm^{-3} for a column density $N(\text{HCO}^+)/\Delta V$ of $3 \times 10^{12} \text{ cm}^{-2} \text{ km}^{-1} \text{ s}$ and a kinetic temperature of 10 K. In particular, we find no evidence for molecular gas density higher than a few 10^4 cm^{-3} on the line of sight to the continuum source. We discuss the implications of our finding on the nature of the molecular gas responsible for the absorption toward Cen A.

Subject headings: galaxies: individual (NGC5128, Cen A) — galaxies: ISM — ISM: molecules — radio lines: galaxies

1. INTRODUCTION

The giant elliptical galaxy NGC 5128 hosts the powerful central radio continuum source Cen A and contains significant amount of gas and dust projected in front of it. It is therefore a good target for absorption study. It was the first radio galaxy in which absorption in neutral hydrogen was detected (Roberts 1970). Since then, numerous molecules have been detected in absorption toward Cen A as well, first at radio wavelengths, such as H₂CO (Gardner & Whiteoak 1976), C₃H₂ (Seaquist & Bell 1986), OH, NH₃ (Seaquist & Bell 1990), and further at millimeter wavelengths with the Swedish-ESO Submillimeter Telescope (SEST): CO, HCO⁺, HCN, HNC, CN, CS (Israel et al. 1990; Eckart et al. 1990; Wiklind & Combes 1997). The molecular absorption profile is best revealed from the HCO⁺(1-0) spectrum published by Wiklind & Combes (1997), owing to the large opacity of the transition, and to the high signal to noise and good spectral resolution of the data.

The HCO⁺(1-0) absorption profile can be mainly decomposed into two components: *i*) a series of narrow (1 – 2 km s⁻¹ wide) lines with absorption depth ranging from ~ 50% to nearly 100% of the continuum intensity, located in the heliocentric velocity range between 540 and 560 km s⁻¹, i.e. close to the systemic velocity, and *ii*) a broad absorption feature between 560 and 640 km s⁻¹, of ~ 10% of the continuum, also including several narrow components (10 to 50% of the continuum). Following Wiklind & Combes (1997), we will refer to these components as Low Velocity Complex (LVC) and High Velocity Complex (HVC), respectively.

Similarly, the HI absorption profile shows numerous narrow components, although some with no molecular counterparts, and vice versa. The estimates of the systemic velocity range between $V_{\text{HEL}} = 536$ and 551 km s^{-1}

in the literature (see e.g. the review by Israel 1998). The existence of redshifted HI absorption, seen only in front of the radio core and not against the inner lobes, has been interpreted by van der Hulst et al. (1983) as gas infall toward the central source. Eventually, this gas infall could be sufficient to fuel a supermassive black hole (van Gorkom et al. 1989). Sarma et al. (2002) showed that a weak and broad HI absorption, previously undetected and corresponding in velocity to the molecular HVC, is occurring only in front of the nucleus. The region showing redshifted gas is limited in size to ≤ 100 pc from the radio core, and is thus a strong candidate for a circumnuclear disk. New HI observations with the Australia Telescope Compact Array (ATCA) allowed Morganti et al. (2008) to also detect blueshifted absorption, thus favoring the interpretation in terms of a rotating circumnuclear disk. It is not clear, however, what is the illuminating background continuum source at this frequency. Indeed, Tingay & Murphy (2001) show that, between 2 and 5 GHz the innermost part of the radio continuum source is affected by free-free absorption that might be caused by circumnuclear ionised gas. The absorption of hard X-ray, indicating a column density of $10^{23} \text{ atoms cm}^{-2}$ of absorbing gas in front of the central source (Evans et al. 2004), also suggests the presence of circumnuclear material around the supermassive black hole, as expected from the AGN unification models (Antonucci 1993).

The central region of Cen A is heavily obscured in the optical, with $A_V \sim 15$ (Israel et al. 1990; Eckart et al. 1990). The presence of a circumnuclear molecular disk in Cen A, with extent of about 100 – 200 pc in radius, has been inferred by several authors (Israel et al. 1990; Hawarden et al. 1993; Rydbeck et al. 1993; Liszt 2001) on the basis of infrared and submillimeter emission data. Recently, Neumayer et al. (2001) mapped the H₂ 2 μm lines emission at $\sim 0.1''$ resolution toward the central region with a field of view of $3'' \times 3''$ ($\sim 50 \times 50$ pc). Their best fit of the H₂ velocity field, using a warped disk model, indicates a median disk inclination angle of $45^\circ \pm 12^\circ$ and a black hole mass of $\sim 5 \times 10^7 M_\odot$.

¹ Academia Sinica, Institute of Astronomy and Astrophysics (ASIAA), P.O. Box 23-141, Taipei 106, Taiwan

² On leave from Center for Quantum Electronics, Institute of Physics, Vietnamese Academy of Science and Technology, 10 DaoTan, ThuLe, BaDinh, Hanoi, Vietnam.

The HVC absorption is significantly redshifted with respect to the systemic velocity, and spread over a larger velocity range than that of the LVC, forming, as seen in the HCO^+ (1-0) line, a broad and continuous absorption over more than 50 km s^{-1} wide. For these reasons, Wiklind & Combes (1997) suggest that the HVC absorption components could originate in the circumnuclear disk. The LVC components, on the other hand, may correspond to intervening gas in the galactic disk of Cen A, although it is difficult to determine their locations. Alternatively, Eckart et al. (1999) proposed that the general velocity structure of the absorption could be explained kinematically with a tilted-ring model and high-altitude clouds, not necessarily requiring the presence of molecular gas close to the active nucleus.

In any case, the physical conditions of the absorbing molecular gas are still poorly known. Previous analysis of CO multi-transition single-dish observations were conducted (Israel et al. 1991), but suffer from strong contamination by line emission. The situation is better for ^{13}CO , as the line emission is greatly reduced. From analysis of the ^{13}CO (1-0) and (2-1) line absorption, Eckart et al. (1990) derived volume density $n(\text{H}_2)$ of a few times 10^4 cm^{-3} for the narrow components in the LVC. Van Langevelde et al. (1995) observed the ground state main lines of OH (rest frequencies of 1665 and 1667 MHz) with the ATCA and estimate similar gas density for LVC absorption components. Interestingly, they also observed the two satellite lines at 1612 and 1720 MHz and find that these lines have a strong conjugate behavior, one in absorption, and the other equally strong in emission. This is particularly remarkable in the HVC, because the corresponding absorption is weak in the main OH lines. Van Langevelde et al. (1995) note that such a behavior could occur at high density $n \gtrsim 10^6 \text{ cm}^{-3}$. To the best of our knowledge, no other molecule has been observed in different rotational transitions, and the physical properties corresponding to the HVC components are mostly unknown.

With the aim to study the properties of the gas in front of the nuclear continuum source, and particularly the dense gas component as a probe of the potential circumnuclear disk, we have observed the high density gas tracers HCO^+ and HCN (3-2) transitions toward the center of Centaurus A with the Submillimeter Array. We present our observations and results in §2 and §3. Implications are discussed in §4. A thorough review on Cen A is given by Israel (1998).

2. OBSERVATIONS AND DATA REDUCTION

The $J = 3 - 2$ transitions of HCO^+ (267.5576 GHz) and HCN (265.8864 GHz) were observed toward Cen A with the Submillimeter Array (SMA), on 2007 April 7th. The array was composed of eight antennas in a compact north-south configuration, optimized for observations of sources in the southern hemisphere. The projected baselines ranged between 5 and 110 m over the course of the observations. The phase reference was set to the position of Cen A at (R.A., Dec.)_{J2000} = ($13^{\text{h}}25^{\text{m}}27^{\text{s}}.60$, $-43^{\circ}01'09''.0$).

We observed Cen A for a total on-source integration time of 4.3 hours. The zenith atmospheric opacity at 225 GHz was between 0.1 and 0.15. System temperatures ranged between 200 and 600 K for the different antennas,

except for one antenna, for which the system temperature was between 600 and 900 K. The data were calibrated with the software package MIR/IDL. The bright radio sources 3C273, 3C279 and Ganymede were observed for bandpass calibration, for which an antenna-based solution was adopted.

The heterodyne receivers were tuned to observe simultaneously the HCO^+ and HCN (3-2) transitions, both placed in the lower sideband (LSB). The $\sim 2 \text{ GHz}$ bandwidth of the LSB was divided into 24 spectral windows (“chunks”), 104 MHz ($\sim 95 \text{ km s}^{-1}$) wide each, and slightly overlapping in frequency.

The continuum emission (Fig.1a) was reconstructed by averaging all the LSB line-free chunks, resulting in a total spectral bandwidth of 1.6 GHz. The absorption components, especially around $V_{\text{HEL}} \sim 550 \text{ km s}^{-1}$, have narrow linewidths ($\sim 1\text{-}5 \text{ km s}^{-1}$). We therefore used a velocity resolution of $\sim 0.2 \text{ km s}^{-1}$ (i.e., 512 channels/chunk) for the chunks corresponding to the HCO^+ and HCN lines. All the other chunks were set to a spectral resolution of 0.8125 MHz (or a velocity resolution of $\sim 0.9 \text{ km s}^{-1}$). To further improve the signal to noise ratio, the spectral resolution of all chunks has been smoothed to 1.625 MHz (i.e., $\sim 1.8 \text{ km s}^{-1}$).

We used the strong and unresolved continuum emission to self-calibrate the line visibilities. We estimate the continuum flux density of Cen A to be $\sim 6.6 \text{ Jy}$ at 266 GHz, with uncertainty of order of 20%, by using Ganymede as a flux calibrator. The complex gains (amplitude and phase *vs* time) were self-calibrated on the continuum visibilities. The amplitude was normalized to the continuum level.

Continuum-subtracted channel maps were produced for both lines. The deconvolved maps, integrated over the LVC (from 535 to 560 km s^{-1}) and HVC (from 565 to 620 km s^{-1}) velocity ranges, are shown in Fig.1c–f. Adopting natural weighting, the uv-coverage of our SMA observations yields a synthesized beam of $4.0'' \times 2.6''$, with a position angle of 9° . A fit of the calibrated line visibilities, with the GILDAS/MAPPING task UVFITS, using a point source model with fixed position (at the phase center) but free amplitude, resulted in the spectra shown in Fig.2.

3. RESULTS

The HCO^+ and HCN (3-2) absorption spectra toward Cen A, obtained with the SMA, are presented in Fig.2. For comparison, we also include the absorption profiles of HCO^+ (1-0) and HI, as parametrized by Wiklind & Combes (1997) and Sarma et al. (2002), respectively.

The HCO^+ (3-2) absorption is clearly detected in the LVC velocity range (see also Fig.1c). A strong and narrow ($\sim 1 \text{ km s}^{-1}$ wide) line, located at $\sim 552 \text{ km s}^{-1}$, matches with the deepest absorption component seen in the HCO^+ (1-0) spectrum. The absorption depth reaches 16% of the continuum level. The r.m.s. noise level, measured over line-free channels, is 2.5% of the continuum. Blueward of this line, at a velocity of 543 km s^{-1} , a second weaker component can be identified and probably results from the blend of several narrow ($\leq 2 \text{ km s}^{-1}$) line components, identified in the high velocity resolution spectrum of Wiklind & Combes (1997). The signal

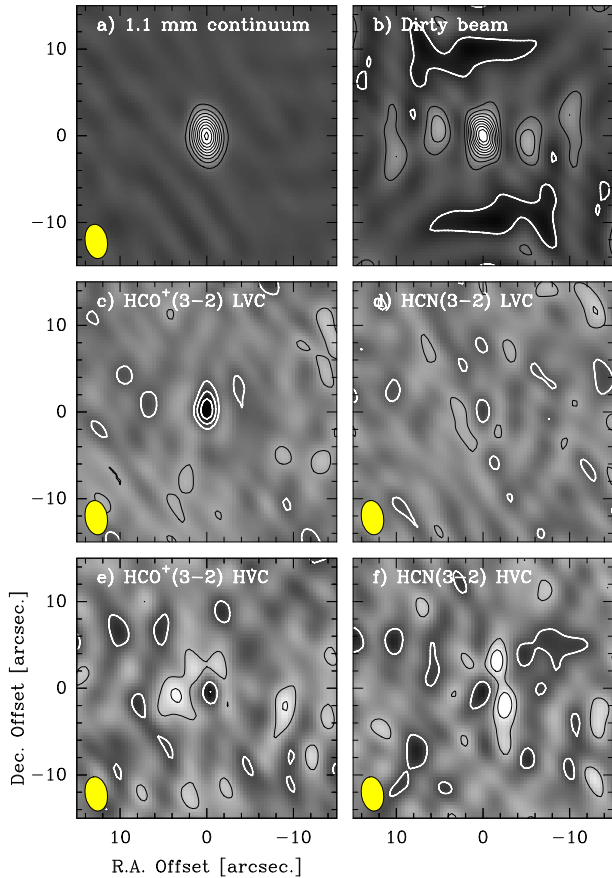


FIG. 1.— a) 1.1 mm normalized continuum emission. Contour levels are drawn every 10% ($\sim 23\sigma$); b) Dirty beam corresponding to the uv-coverage of our SMA observations (contour levels every 10%, in black for positive contours and white for negative ones); c,d,e,f) Maps of the HCO⁺ and HCN(3-2) line intensity integrated over the LVC and HVC velocity ranges. The continuum emission has been subtracted from visibilities before imaging. Contour levels are shown every 2σ , i.e., $1.2 \text{ Jy beam}^{-1} \text{ km s}^{-1}$ for LVC maps and $1.8 \text{ Jy beam}^{-1} \text{ km s}^{-1}$ for HVC maps, in black for positive contours and white for negative ones. The synthesized beam ($4.0'' \times 2.6''$, P.A. = 9°) is shown at the bottom left corner of each map.

to noise ratio of this feature, however, is limited, and barely reaches 3σ at the peak.

Concerning the HCN (3-2) line, we tentatively detect counterparts to the 543 and 552 km s^{-1} components, although the signal to noise ratio is poor, with maximum absorption of $\sim 7\%$. We note that the hyperfine structure of the HCN (3-2) transition concentrates about 93% of the total line intensity within 0.3 MHz (e.g., Maki 1974), and is therefore not resolved given our spectral resolution.

Given the rms noise level of our observations, $\sim 2.5\%$ of the continuum level, we do not detect any other absorption feature. Especially, no counterparts of the HVC components are detected. Also, no HCO⁺ or HCN (3-2) emission is evident.

4. DISCUSSION

4.1. Continuum background and filling factor

The 266 GHz continuum emission remains unresolved at our angular resolution of $\sim 3''$. From Very Long Baseline Interferometry (VLBI), the nuclear region of Cen A is shown to harbor a core-jet radio structure

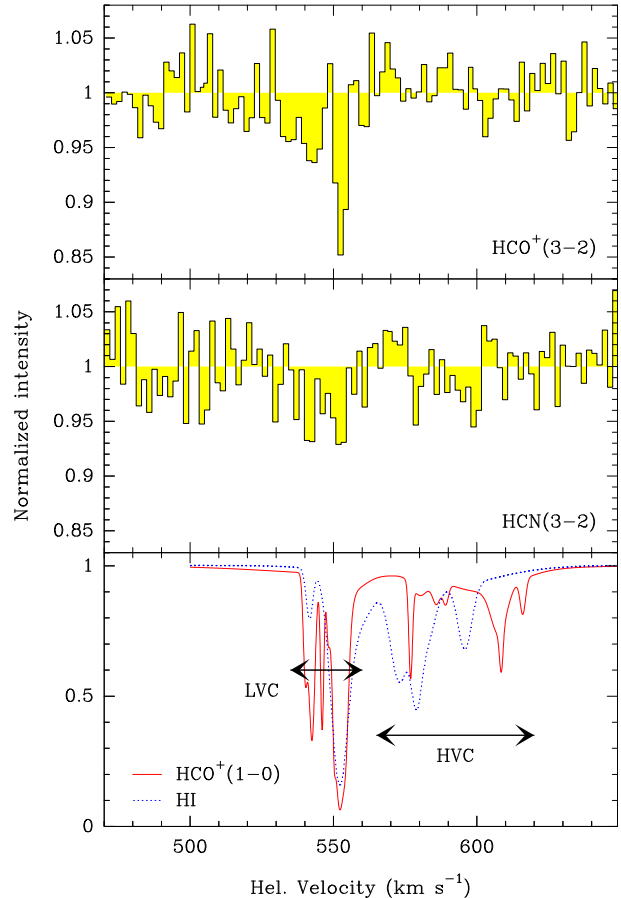


FIG. 2.— Spectra of the HCO⁺ (top) and HCN (middle) (3-2) absorption lines toward Cen A. The velocity resolution is $\sim 1.8 \text{ km s}^{-1}$. The profile of the HCO⁺ (1-0) (full line, observed by Wiklind & Combes 1997) and HI absorptions (dotted, obtained by Sarma et al. 2002) are shown in the bottom frame. The velocity range of the LVC and HVC is also indicated.

(Tingay et al. 1998). As the jet has a steep radio spectrum, with negligible flux at millimeter wavelengths, the molecular absorption should however occur toward the radio core. Kellermann et al. (1997) measured the size of the radio core as $0.5 \pm 0.1 \text{ mas}$ in diameter from 43 GHz VLBI observations, corresponding to a linear dimension of $\sim 0.01 \text{ pc}$, and yielding a brightness temperature on the order of 10^{10} K . The temperature of any molecular gas in the line of sight is therefore expected to be completely negligible with respect to that of the continuum. Given the very small apparent size of the continuum source at millimeter wavelengths, we expect the continuum source to be completely covered by the absorbing clouds, and will assume a filling factor of unity in our analysis. This assumption is supported by VLBA data of the OH 18 cm absorption, which appears to cover a large fraction the continuum source (van Langevelde et al. 2005).

In the following, we will compare our HCO⁺ and HCN (3-2) data to previous observations of the corresponding (1-0) transitions obtained in 1995-1996 by Wiklind & Combes (1997). To the best of our knowledge, no other observations of HCO⁺ or HCN absorption toward Cen A were attempted inbetween. The comparison might thus be affected by time variations, although Wiklind & Combes (1997) could not detect significant

changes of more than 10% between their HCO⁺ (1-0) absorption profile and that observed 7 years before by Eckart et al. (1990).

4.2. Excitation analysis

In order to study the excitation conditions of the HCO⁺ and HCN (3-2) lines in the line of sight to Cen A, we have used a molecular excitation code based on the large velocity gradient (LVG) approximation. Molecular data for HCO⁺ and HCN, including the energy levels, the radiative transition rates and collisional cross sections, were taken from the Leiden Atomic and Molecular Database (Schöier et al. 2005). In our calculations, we include all rotational levels up to the $J = 10$ level. The temperature of the cosmic background radiation field is set to 2.73 K. Our code need three basic parameters as inputs: the molecular hydrogen density $n(\text{H}_2)$, the kinetic temperature T_{kin} and the gas column density per unit velocity $N/\Delta V$. The statistical equilibrium equations setup in the framework of the LVG approximation are solved iteratively using a Newton-Raphson method. We consider that convergence is achieved when the relative change in level populations is less than 10^{-3} between two successive iterations.

We present the results of our calculations in Fig.3 and 4, where the changes of excitation temperature and line opacity as a function of molecular hydrogen density are shown for the $J = 1 - 0$, $J = 2 - 1$ and $J = 3 - 2$ transitions of HCO⁺ and HCN molecules, respectively. We assume a kinetic temperature of 10 K, within the range of temperatures commonly inferred in previous studies (Israel et al. 1991; Eckart et al. 1990). The column density per unit velocity is set to $3 \times 10^{12} \text{ cm}^{-2} \text{ km}^{-1} \text{ s}$ for HCO⁺, and $2 \times 10^{12} \text{ cm}^{-2} \text{ km}^{-1} \text{ s}$ for HCN, respectively. These values are consistent with that derived by Wiklind & Combes (1997).

At low gas density, i.e., $n(\text{H}_2) \sim 10^3 \text{ cm}^{-3}$, the HCO⁺ molecules are not excited to high J levels. As can be seen from Fig.3, the excitation temperature is low for all transitions shown. Most of the HCO⁺ molecules stay in the $J = 0$ and $J = 1$ levels, resulting in high opacity for the $J = 1 - 0$ and $2 - 1$ transitions. As the gas density increases, more HCO⁺ molecules are excited to higher J levels. The opacity of the $J = 1 - 0$ transition drops rapidly, while the opacity of the $J = 3 - 2$ transition increases at nearly the same pace. We note here the non-intuitive behaviour of the $J = 2 - 1$ transition: the opacity of this transition increases slightly with density, peaking at a hydrogen density of 10^5 cm^{-3} and then falls off at higher density. The $J = 2 - 1$ line opacity remains optically thick for the whole range of density considered in our calculations. When the gas density reaches a few 10^5 cm^{-3} , the opacity of both the $J = 1 - 0$ and $J = 3 - 2$ lines becomes comparable. At high gas density, greater than a few times 10^6 cm^{-3} , all the three lines are thermalized. In this case, the opacity of the lines are determined by the usual Boltzmann distribution of level population. As we can see from Fig.3, the $J = 3 - 2$ line has a significantly higher opacity than the $J = 1 - 0$ line. From the behaviour of the line opacity as a function of gas density, we suggest that the comparison of opacity for the $J = 1 - 0$ and $J = 3 - 2$ pair constitutes a sensitive constraint to the gas density.

The excitation temperature and line opacity for HCN molecules behave in a similar way (Fig.4). However, the HCN lines become thermalized at higher density, above 10^7 cm^{-3} , due to lower collision rates in comparison to that of HCO⁺.

For completeness, we also calculate the excitation temperature and opacity as a function of the column density of HCO⁺ for a gas density of $n(\text{H}_2) = 10^4 \text{ cm}^{-3}$ and a kinetic temperature of 10 K (see Fig.5). The opacity of the three transitions increases monotonically with the HCO⁺ column density. Especially, the HCO⁺ (3-2) transition shows appreciable opacity ($\tau \gtrsim 0.1$) only above $N(\text{HCO}^+)/\Delta V > 10^{12} \text{ cm}^{-2} \text{ km}^{-1} \text{ s}$, where the (1-0) and (2-1) transitions become rapidly optically thick. The comparison of the opacity for the $J = 1 - 0$ and $3 - 2$ transitions of HCO⁺ thus gives useful informations on the column density of absorbing gas.

4.3. IR excitation

So far, we have neglected the effect of the infrared radiation field emitted by dust particles, on the excitation of the HCN and HCO⁺ molecules. Both molecules can be excited from the ground state $J = 0$ to the $J = 1$ rotational level of the first bending mode $\nu_2 = 1$ by the absorption of IR photons at $14 \mu\text{m}$ for HCN and $12 \mu\text{m}$ for HCO⁺. Subsequent decay transfers a fraction of the excited molecules to the $J = 3$ level of the ground state.

The strength of the local radiation field at the location where the absorption arises is still poorly known. Van Langevelde et al. (1995) adopt a representative radiation field consisting of two components: a warm dust component at a temperature of 150 K and a cooler dust component at 43 K. Obviously, only the warm dust component contributes to the IR radiation at the absorption wavelengths of HCN and HCO⁺ molecules.

We have repeated our LVG calculations for the HCN molecule taking directly into account the IR pumping. The formulae for the excitation and de-excitation rates are taken from Deguchi & Uyemura (1984). Results are shown in Figure 4. Because of IR pumping, the excitation temperatures of all rotational transitions increase noticeably in comparison to the case without IR pumping for gas densities below 10^6 cm^{-3} . At higher densities approaching 10^7 cm^{-3} , the effect of IR pumping is very small, as expected. We note that at low gas densities, where more molecules are excited by IR pumping to higher J levels, there is an increase in the opacity of the $J = 3 - 2$ transition while the opacity of $J = 1 - 0$ transition is reduced. Interestingly, the opacity of $J = 2 - 1$ transition remains approximately the same as in the case without IR pumping. Because both HCN and HCO⁺ molecules have similar transition probability (García-Burillo et al. 2006) and vibrational transition frequency, we expect very similar results for the excitation of HCO⁺ molecules. It is clear from Figure 4 that with or without the IR pumping the behavior of the line opacity as a function of the gas density does not change qualitatively. Observationally, the $J = 3 - 2$ absorption of HCO⁺ and HCN is very weak, suggesting that the IR pumping probably does not play an important role in the excitation of these molecules. Therefore our conclusion in the previous section is not affected by IR pumping.

4.4. Physical conditions for the LVC components

The LVC components, i.e., between $V_{\text{HEL}} = 535$ and 560 km s^{-1} , all exhibit strong absorption in the HCO⁺ (1-0) transition with opacities $\gtrsim 1$, whereas our SMA data shows that the HCO⁺ (3-2) absorption of the same features is relatively weak, with opacities $\lesssim 0.2$. From Fig.3, we can thus estimate that, in order to be consistent with the observations, the density of the absorbing gas should be about 10^4 cm^{-3} for a HCO⁺ column density per velocity unit on the order of $3 \times 10^{12} \text{ cm}^{-2} \text{ km}^{-1} \text{ s}$.

Similarly, the HCN (1-0) absorption components reach an opacity of about 0.9, while our tentative detection of HCN (3-2) absorption suggests opacity well below 0.1. This is also consistent with gas density of about 10^4 cm^{-3} and column density per velocity unit of $\sim 2 \times 10^{12} \text{ cm}^{-2} \text{ km}^{-1} \text{ s}$ (Fig.4).

Our results are therefore comparable to that obtained by Eckart et al. (1990) from analysis of the ¹²CO and ¹³CO (1-0) and (2-1) lines for the deepest absorption feature at $V_{\text{HEL}} = 552 \text{ km s}^{-1}$. They estimate a kinetic temperature of no more than 10 K and a gas density of around $2 \times 10^4 \text{ cm}^{-3}$. They also note, however, that the hyperfine structure line ratios for the HCN and CN (1-0) transitions could suggest a clumpy medium, with density possibly up to 10^6 cm^{-3} . We do not see evidence of such high density medium from our data.

4.5. Constraints for the HVC components

The main goal of these observations was to probe the physical properties of the gas associated with the HVC absorption, possibly associated with the circumnuclear disk around the supermassive black hole in Cen A. The HVC absorption is best detected in HCO⁺ (1-0), but also appears in HI (although with no one to one correspondence, see e.g. Sarma et al. 2002), OH ground state lines (van Langevelde et al. 1995), HCN and HNC (1-0), and CS (2-1) lines (Wiklind & Combes 1997).

According to the results of our excitation analysis, the non-detection of HCO⁺ (3-2) absorption counterpart to HCO⁺ (1-0) components suggests that the gas density is lower than a few times 10^4 cm^{-3} .

Eckart et al. (1999) proposed a kinematical explanation for the HVC absorption, which could be caused by clouds located at large galactocentric radii on the order of 0.5 kpc and high altitude of $\sim 300 \text{ pc}$ above the disk. Whereas our observations give constraints on the physical conditions of the molecular gas, particularly on density, they alone can not rule out the existence of a circumnuclear disk neither confirm the kinematic interpretation of the complex absorption system.

5. CONCLUSIONS

We have observed the absorption from the HCO⁺ and HCN (3-2) transition toward the center of Centaurus A with the Submillimeter Array. At least two absorption components are identified in the HCO⁺ (3-2) spectrum. A first narrow component, located at $V_{\text{HEL}} \sim 552 \text{ km s}^{-1}$, reaches a depth of about 16% of the continuum level and corresponds to the deepest absorption component observed in other molecules and HI. A second weak component, approximately 10 km s^{-1} blueward and 7% deep, probably corresponds to the blend of several narrow components identified in the HCO⁺ (1-0) spectrum by Wiklind & Combes (1997). Given our sensitivity of 2.5% of the continuum level, no counterparts of the redshifted absorption components seen in HCO⁺ (1-0) between 570 and 620 km s^{-1} are detected. Absorption from the HCN (3-2) transition is tentatively detected around $V_{\text{HEL}} \sim 552 \text{ km s}^{-1}$.

While the sensitivity and dynamic range of our SMA observations are limited, the weak absorption in the HCO⁺ and HCN (3-2) transitions, as compared to the corresponding $J = 1 - 0$ absorption, provides useful informations about the physical conditions of the absorbing gas. We have performed a simple excitation analysis for the $J = 1 - 0$, $2 - 1$ and $3 - 2$ transitions of HCO⁺ and HCN molecules. We find that the HCO⁺ (1-0) and (3-2) pair of transitions is an excellent indicator of the absorbing gas density. Absorption components close to the systemic velocity (LVC) have density on the order of a few times 10^4 cm^{-3} , for a column density of a few times 10^{12} cm^{-2} . The non-detection of absorption counterparts to the HVC redshifted components suggests corresponding density of 10^4 cm^{-3} or lower. Thus, nowhere on the line of sight to the central continuum source of Cen A is to be found molecular gas with density higher than a few 10^4 cm^{-3} . The inclusion of IR excitation in our model does not change substantially these results. Either the line of sight to the radio continuum source does not intersect the circumnuclear disk, and the different absorption components arise at different loci in the galactic disk, or the density of the absorbing gas in the circumnuclear disk is lower than a few 10^4 cm^{-3} .

We thank the SMA staff for their very competent assistance with these observations. We are grateful to the anonymous referee for providing us with constructive comments. The Submillimeter Array is a joint project between the Smithsonian Astrophysical Observatory and the Academia Sinica Institute of Astronomy and Astrophysics and is funded by the Smithsonian Institution and the Academia Sinica.

Facility: Submillimeter Array

REFERENCES

- Antonucci, R., 1993, ARA&A, 31, 473
 Deguchi, S. & Uyemura, M., 1984, ApJ, 285, 153
 Eckart, A., Cameron, M., Genzel, R., et al., 1990, ApJ, 365, 522
 Eckart, A., Wild, W. & Ageorges, N., 1999, ApJ, 516, 769
 Evans, D. A., Kraft, R. P., Worrall, D. M., et al., 2004, ApJ, 612, 786
 García-Burillo, S., Graciá-Carpio, J., Guélin, M., et al., 2006, ApJ, 645, L17
 Gardner, F. F. & Whiteoak, J. B., 1976, MNRAS, 175, 9
 Hawarden, T. G., Sandell, G., Matthews, H. E., et al., 1993, MNRAS, 260, 844
 Israel, F. P., van Dishoeck, E. F., Baas, F., et al., 1990, A&A, 227, 342
 Israel, F. P., van Dishoeck, E. F., Baas, F., et al., 1991, A&A, 245, L13
 Israel, F. P., 1998, A&A Rev., 8, 237
 Kellermann, K. I., Zensus, J. A. & Cohen, M. H., 1997, ApJ, 475, L93
 Maki, A. G., 1974, J. Phys. Chem. Ref. Data, Vol. 3, p. 221
 Liszt, H., 2001, A&A, 371, 865
 Morganti, R., Oosterloo, T., Struve, C. & Saripalli, L., 2008, A&A, 485, L5

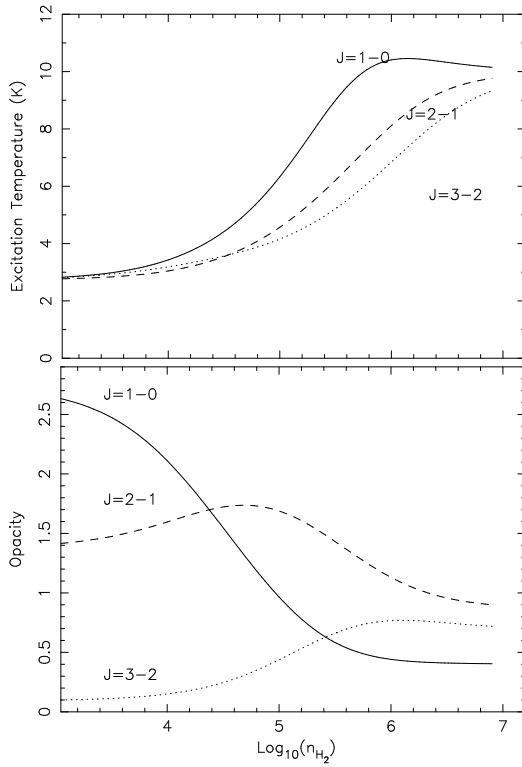


FIG. 3.— Excitation temperature and opacity of the $J = 1 - 0$, $2 - 1$ and $3 - 2$ transitions of HCO^+ as a function of gas density in the case $T_{\text{kin}} = 10$ K and $N(\text{HCO}^+)/\Delta V = 3 \times 10^{12} \text{ cm}^{-2} \text{ km}^{-1} \text{ s}$.

Neumayer, N., Cappellari, M., Reunanen, J., et al., 2007, *ApJ*, 671, 1329
 Rydbeck, G., Wiklind, T., Cameron, M., et al., 1993, *A&A*, 270, L13
 Roberts, M. S., 1970, *ApJ*, 161, L9
 Sarma, A. P., Troland, T. H. & Rupen, M. P., 2002, *ApJ*, 564, 696
 Schöier, F. L., van der Tak, F. F. S., van Dishoeck, E. F., & Black, J. H., *A&A*, 432, 369
 Seaquist, E. R. & Bell, M. B., 1986, *ApJ*, 303, L67
 Seaquist, E. R. & Bell, M. B., 1990, *ApJ*, 364, 94
 Tingay, S. J., Jauncey, D. L., Reynolds, J. E., et al., 1998, *AJ*, 115, 960

Tingay, S. J. & Murphy, D. W., 2001, *ApJ*, 546, 210
 van der Hulst, J. M., Golisch, W. F. & Haschick A. D., 1983, *ApJ*, 264, L37
 van Gorkom, J. H., Knapp, G. R., Ekers, R. D., et al., 1989, *AJ*, 97, 708
 van Langevelde, H. J., van Dishoeck, E. F., Sevenster, M. N. & Israel, F. P., 1995, *ApJ*, 448, L123
 van Langevelde, H. J.; Pihlström, Y. & Beasley, A., 2005, *Ap&SS*, 295, 249
 Wiklind, T. & Combes, F., 1997, *A&A*, 324, 51

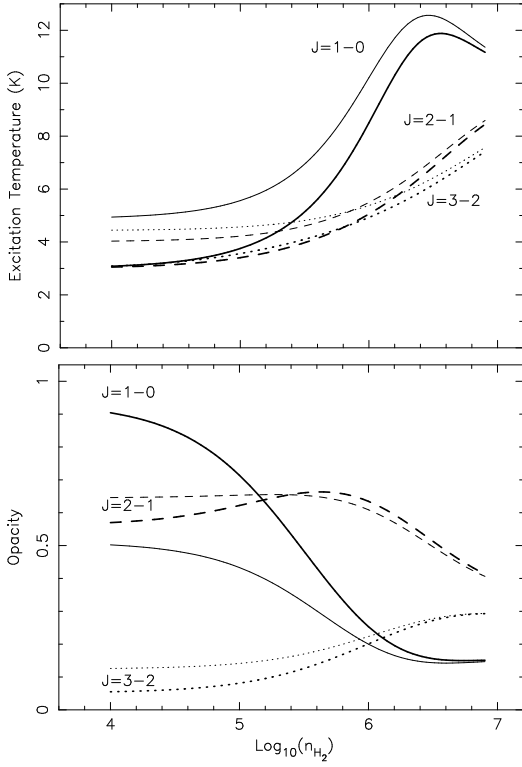


FIG. 4.— Excitation temperature and opacity of the $J = 1 - 0$, $2 - 1$ and $3 - 2$ transitions of HCN as a function of gas density in the case $T_{\text{kin}} = 10$ K and $N(\text{HCN})/\Delta V = 2 \times 10^{12} \text{ cm}^{-2} \text{ km}^{-1} \text{ s}$. Thick curves correspond to the case of excitation by collision only, thin curves with IR pumping included. The parameters of the radiation field are taken from van Langevelde et al. (1995): $T_D = 150$ K, $\Delta\Omega = 0.1$, $E(B - V) = 1$ and $\beta = 1$.

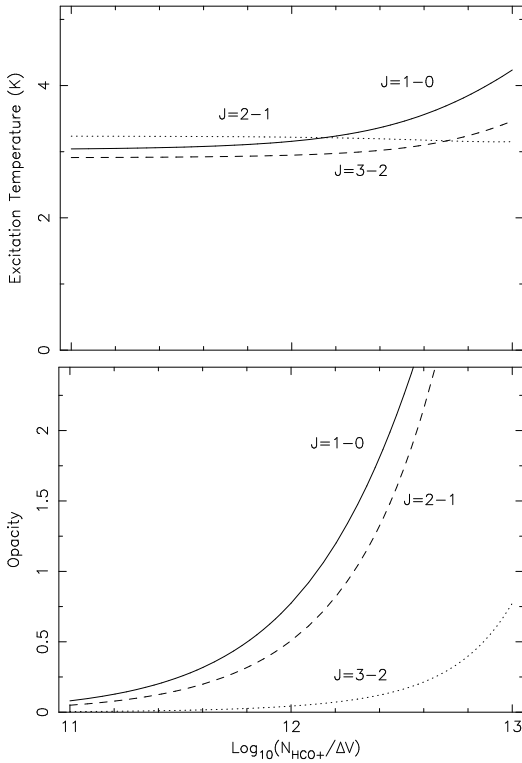


FIG. 5.— Excitation temperature and opacity for the $J = 1 - 0$, $2 - 1$ and $3 - 2$ transitions of HCO⁺ for a gas density of $n(\text{H}_2) = 10^4 \text{ cm}^{-3}$ and a kinetic temperature of $T_{\text{kin}} = 10$ K.